Eur. Phys. J. Spec. Top. (2022) 231:2183–2197
https://doi.org/10.1140/epjs/s11734-021-00369-6

THE EUROPEAN PHYSICAL JOURNAL SPECIAL TOPICS

Regular Article

Chaos threshold analysis of Duffing oscillator with fractional-order delayed feedback control

Shaofang Wen[1,a], Hao Qin[1], Yongjun Shen[2], and Jiangchuan Niu[2]

[1] State Key Laboratory of Mechanical Behavior and System Safety of Traffic Engineering Structures, Shijiazhuang Tiedao University, Shijiazhuang 050043, China
[2] School of Mechanical Engineering, Shijiazhuang Tiedao University, Shijiazhuang 050043, China

Received 19 May 2021 / Accepted 7 December 2021 / Published online 20 January 2022

Abstract In this paper, the bifurcation and chaotic threshold of Duffing oscillator with fractional-order delayed feedback control is studied. The fractional-order delayed feedback control is equivalent to the approximate integer-order control. It is found that the fractional-order delayed feedback control has the function of displacement feedback and velocity feedback. Then, the analytically necessary condition for generating chaos in Duffing oscillator with fractional-order delayed feedback control is obtained by Melnikov method. The accuracy of the analytically necessary condition by Melnikov method is verified by numerical simulation and the largest Lyapunov exponents of the system. From the analysis of the numerical simulation results, it is found that there are two paths leading to the chaos after period-doubling bifurcations due to different initial values in Duffing oscillator with fractional-order delayed feedback. Finally, the influence of the parameters of the fractional-order delayed feedback control on bifurcation and chaos is analyzed. The increase of the fractional-order delayed feedback gain will resist the generation of chaos. Both time delay and the fractional-order affect the threshold of chaos in the form of trigonometric functions. The better control performance in the system can be obtained by choosing the reasonable fractional order and time delay. Those results present some new system characteristics which provide theoretic guidance to design and control of this kind system.

1 Introduction

It is well known that bifurcation and chaos phenomenon is a unique motion in nonlinear systems. When bifurcation and chaos occur, the dynamical characteristics of the system will change, such as period, amplitude and stability. A series of engineering problems in the system with nonlinear factors will be caused by bifurcation and chaos. The control of bifurcation and chaos is a technical challenge. At first, scholars generally believed that chaos could not be controlled [1,2]. Until 1990, Ott et al. [3] put forward OGY method to control chaos, which made the research on chaos control become a hot research field. After that, many control methods on bifurcation and chaos have been put forward by scholars. Li et al. [4] investigated the dynamical behaviors of an improved wheelset model with two degrees of freedom, then the adaptive feedback control and linear feedback control were used to control the chaos and bifurcation of the wheelset system. Saghafi et al. [5] studied a control system to eliminate homoclinic bifurcation and chaos of a gear system, and obtained the analytical solution of the gear system with the external control excitation based on Melnikov method. Shiva et al. [6] studied the stability and bifurcation of a new chaotic fractional-order system, and used linear feedback control technology to eliminate the chaotic vibration of a new fractional-order system. Wang et al. [7] proposed an adaptive intermittent control method to realize the synchronization of time-delay chaotic system. Chen et al. [8] proposed a nonlinear feedback controller to make the two chaotic Genesio systems synchronize and simplify the stability analysis of the controlled system.

It is well known that time delays are unavoidable. In the dynamical control system, the time delay is produced by the delay of signal transmission. This kind of delay is uncertain, which will change the dynamical characteristic of the system and even lead to the change of the system phenomena such as bifurcation and chaos [9–14]. With the development of science and the demand for high precision in engineering, the model more closer to the reality is needed to get a higher precision control effect in dynamics research, so time delay introduced into the dynamic model is necessary, which has a wide application background [15]. Yu et al. [16] analyzed the dynamical characteristics of Van der Pol–Duffing fast-slow oscillator controlled by parametric delay feedback. Xu et al. [17] investigated the effect of time delay on the dynamics of the Van der Pol–Duffing

[a] e-mail: wsf39811@163.com (corresponding author)

oscillator with linear and nonlinear time-delayed position feedback. Feng et al. [18] studied the first-passage failure of Duffing oscillator with the delayed feedback control under the combined harmonic and white-noise excitation based on the stochastic averaging method. Then the effects of time delay on the system dynamical characteristics are investigated. Cai et al. [19] used Melnikov technique to analyze a nonautonomous time-delay feedback control system, and obtained the conclusion that the delay time of chaotic attractor is independent of the period of inherent unstable orbit.

Duffing equation is one of the most common and typical models, which can simulate a large number of structures in engineering fields. Scholars have carried out many researches on the equation itself and its derivative system, in which the fractional-order system has attracted more and more attention [20–24]. Fractional calculus was proposed about 300 years ago. In recent years, fractional calculus develops extremely fast and it is widely used in many interdisciplinary branches of science due to its effectiveness in describing and investigating complicated phenomena [21,25–27]. At present, the application of fractional calculus in engineering field can be divided into two categories. The first, fractional calculus is used to accurately model the engineering materials between ideal solid and ideal fluid, which can reflect the constitutive relationship of materials more truly. The other is the fractional-order control based on fractional calculus, which can improve the control effect of the control system based the advantages of good robustness and strong antinoise ability of fractional calculus feedback. Wang et al. [28] studied the chaos synchronization between two different uncertain fractional-order chaotic systems with disturbance based on fractional-order Lyapunov stability analysis method, and proposed adaptive sliding mode control design procedure. Wei et al. [29] proposed a robust adaptive control scheme through the backstepping procedure to deal with the time-varying disturbance of asymmetric fractional-order systems. Chen et al. [30] advanced a sliding-mode controller for a class of fractional-order uncertain linear perturbed systems based on the linear matrix inequality and the stability theory of fractional-order nonlinear systems.

Melnikov method is a kind of first-order approximate method to analyze the necessary condition for chaos in a dynamical system. It was originally used to prove the existence of homoclinic orbit or heteroclinic orbit, and now it is widely used to judge the necessary condition for chaos of the integer-order system. At present, there is no literature on the analysis of fractional-order delayed feedback control system by Melnikov method.

In this paper, the chaos threshold analysis of Duffing oscillator with fractional-order delayed feedback control is presented by Melnikov method. In Sect. 2, the fractional-order delayed feedback control term is investigated, and the first-order approximate analytical results of the fractional-order delayed feedback control are obtained. The equivalent linear damping and equivalent linear stiffness are used to transform the fractional-order term into trigonometric function and exponential function, so that the fractional-order system is equivalent to the approximate integer-order system. In addition, the approximate analytical solution of the necessary conditions for chaos generation of Duffing oscillator with fractional-order delayed feedback control is derived based on Melnikov method. In Sect. 3, the threshold value of chaos in Duffing system with fractional-order delayed feedback is calculated by the numerical iteration method, and the results of the numerical solution are compared with the analytical results to verify the correctness and satisfactory precision of the approximate analytical solution. Then, the influence of fractional-order delayed feedback control parameters on the bifurcation and chaos of the system is studied by using the obtained analytical results in Sect. 4. At last, the main conclusions are made.

2 Approximate analytical solution of the necessary condition for chaos

In this section, Duffing oscillator with fractional-order delayed feedback control is considered. The system is as follows

$$\ddot{x} - kx + c\dot{x} + \alpha x^3 = f\cos(\omega t) - \lambda D_t^p x(t-\tau), \quad (1)$$

where k, c, α, f and ω are the linear stiffness coefficient, the linear damping coefficient, the nonlinear stiffness coefficient, the excitation amplitude, and excitation frequency respectively. $\lambda D_t^p x(t-\tau)$is the fractional-order delayed feedback control. It is the p-order derivative of $x(t-\tau)$ to t with the feedback coefficient λ and the time delay τin control procedure. All the parameters of the system are positive and dimensionless. There are several definitions for fractional-order derivative, such as Grünwald–Letnikov, Riemann–Liouville and Caputo definitions [25,26]. In a broad senses, they are equivalent for most mathematical functions. Accordingly, Caputo's definition is adopted with the form as

$$D_t^p[x(t)] = \frac{1}{\Gamma(1-p)}\int_0^t \frac{x'(u)}{(t-u)^p}\mathrm{d}u, \quad (2)$$

where $\Gamma(n)$ is Gamma function.

Supposing the solution of Eq. (1) is expressed as

$$x(t) = \alpha\cos(\omega t + \theta) \quad (3a)$$
$$\dot{x}(t) = -\alpha\omega\sin(\omega t + \theta), \quad (3b)$$

and it can be obtained

$$x(t-\tau) = \alpha\cos[\omega(t-\tau) + \theta] \quad (3c)$$
$$\dot{x}(t-\tau) = -\alpha\omega\sin[\omega(t-\tau) + \theta]. \quad (3d)$$

Substituting Eq. (3a) into the fractional-order delayed feedback term based on Caputo's definition, one could

obtain

$$D_t^p[x(t-\tau)] = \frac{-\alpha\omega}{\Gamma(1-p)}\int_0^t \frac{\sin(\omega u+\theta)}{(t-\tau-u)^p}\mathrm{d}u \tag{4}$$

Define $s = t-\tau-u$, Eq. (4) becomes

$$\begin{aligned}
&D^p[x(t-\tau)]\\
&= \frac{-\alpha\omega}{\Gamma(1-p)}\int_t^0 -\frac{\sin(\omega(t-\tau-s)+\theta)}{s^p}\mathrm{d}s\\
&= \frac{-\alpha\omega}{\Gamma(1-p)}\int_0^t \frac{\sin(\omega(t-\tau-s)+\theta)}{s^p}\mathrm{d}s\\
&= \frac{-\alpha\omega\cos\theta}{\Gamma(1-p)}\int_0^t \frac{\sin(\omega(t-\tau-s))}{s^p}\mathrm{d}s - \frac{\alpha\omega\sin\theta}{\Gamma(1-p)}\\
&\quad\times\int_0^t \frac{\cos(\omega(t-\tau-s))}{s^p}\mathrm{d}s\\
&= \frac{-\alpha\omega\cos\theta}{\Gamma(1-p)}\left\{\sin[\omega(t-\tau)]\int_0^t \frac{\cos(\omega s)}{s^p}\mathrm{d}s\right.\\
&\quad\left.-\cos[\omega(t-\tau)]\int_0^t \frac{\sin(\omega s)}{s^p}\mathrm{d}s\right\}\\
&\quad-\frac{\alpha\omega\sin\theta}{\Gamma(1-p)}\left\{[\cos[\omega(t-\tau)]\int_0^t \frac{\cos(\omega s)}{s^p}\mathrm{d}s\right.\\
&\quad\left.+\sin[\omega(t-\tau)]\int_0^t \frac{\sin(\omega s)}{s^p}\mathrm{d}s\right\}\\
&= \frac{-\alpha\omega}{\Gamma(1-p)}\left\{\sin[\omega(t-\tau)+\theta]\int_0^t \frac{\cos(\omega s)}{s^p}\mathrm{d}s\right.\\
&\quad\left.-\cos[\omega(t-\tau)+\theta]\int_0^t \frac{\sin(\omega s)}{s^p}\mathrm{d}s\right\}
\end{aligned} \tag{5}$$

According to the two basic formulas in Ref. [21]

$$\begin{aligned}
&\int_0^t \frac{\sin(\omega s)}{(s)^p}ds\\
&= \omega^{p-1}\left[\Gamma(1-p)\cos\left(\frac{p\pi}{2}\right) - \frac{\cos\omega t}{(\omega t)^p} + \mathrm{O}[(\omega t)^{-p-1}]\right]
\end{aligned} \tag{6a}$$

$$\begin{aligned}
&\int_0^t \frac{\cos(\omega s)}{(s)^p}\mathrm{d}s\\
&= \omega^{p-1}\left[\Gamma(1-p)\sin\left(\frac{p\pi}{2}\right) + \frac{\sin\omega t}{(\omega t)^p} + \mathrm{O}[(\omega t)^{-p-1}]\right].
\end{aligned} \tag{6b}$$

Substituting Eq. (6) into Eq. (5), one can get

$$\begin{aligned}
&D_t^p[x(t-\tau)]\\
&= -\alpha\omega\sin[\omega(t-\tau)+\theta]\omega^{p-1}\\
&\quad\times\left[\sin\left(\frac{p\pi}{2}\right) + \frac{\sin\omega t}{\Gamma(1-p)(\omega t)^p} + \frac{O[(\omega t)^{-p-1}]}{\Gamma(1-p)}\right]\\
&\quad+\alpha\omega\cos[\omega(t-\tau)+\theta]\omega^{p-1}\\
&\quad\times\left[\cos\left(\frac{p\pi}{2}\right) + \frac{\cos\omega t}{\Gamma(1-p)(\omega t)^p} + \frac{O[(\omega t)^{-p-1}]}{\Gamma(1-p)}\right]
\end{aligned} \tag{7}$$

The steady-state dynamical performance of the system after repeated vibration is focused in this paper, so the higher-order terms of Eq. (7) are omitted, and the first-order approximate result is

$$\begin{aligned}
D_t^p[x(t-\tau)] &= -\alpha\omega\sin[\omega(t-\tau)+\theta]\omega^{p-1}\sin\left(\frac{p\pi}{2}\right)\\
&\quad+\alpha\omega\cos[\omega(t-\tau)+\theta]\omega^{p-1}\cos\left(\frac{p\pi}{2}\right)\\
&= -\alpha\omega\left[\sin(\omega t+\theta)\cos\omega\tau\sin\frac{p\pi}{2} - \cos(\omega t+\theta)\right.\\
&\quad\left.\times\sin\omega\tau\sin\frac{p\pi}{2}\right]\omega^{p-1}\\
&\quad-\alpha\omega\left[-\cos(\omega t+\theta)\cos\omega\tau\cos\frac{p\pi}{2} - \sin(\omega t+\theta)\right.\\
&\quad\left.\times\sin\omega\tau\cos\frac{p\pi}{2}\right]\omega^{p-1}\\
&= -\alpha\omega\sin(\omega t+\theta)\omega^{p-1}\sin\left(\frac{p\pi}{2}-\omega\tau\right)\\
&\quad+\alpha\omega\cos(\omega t+\theta)\omega^{p-1}\cos\left(\frac{p\pi}{2}-\omega\tau\right)
\end{aligned} \tag{8}$$

Substituting the system original parameters into Eq. (8), one can get

$$\begin{aligned}
D_t^p[x(t-\tau)] &= \omega^{p-1}\sin\left(\frac{p\pi}{2}-\omega\tau\right)\dot{x}(t)\\
&\quad+\omega^p\cos\left(\frac{p\pi}{2}-\omega\tau\right)x(t)
\end{aligned} \tag{9}$$

To verify the accuracy of the first-order approximate result of the fractional-order delayed feedback term, the amplitude–frequency responses of the Duffing oscillator Eq. (1) is investigated based on the numerical method and the first-order approximate result, respectively, which are shown in Fig. 1. It could be found that the results of the two methods are consistent, which verified the correctness of the first-order approximate result.

Substituting Eq. (9) into Eq. (1), one could obtain

$$\begin{aligned}
\ddot{x} - kx + c\dot{x} + \alpha x^3 &= f\cos(\omega t)\\
&\quad-\lambda\left[\omega^{p-1}\sin\left(\frac{p\pi}{2}-\omega\tau\right)\dot{x}\right.\\
&\quad\left.+\omega^p\cos\left(\frac{p\pi}{2}-\omega\tau\right)x\right]
\end{aligned} \tag{10}$$

From Eq. (9), it could be found that the fractional-order delayed feedback term can be equivalent to the form of trigonometric function and exponential function. That is to say, the fractional-order differential term plays the role of damping and stiffness at the same time, which can be equivalent to the equivalent linear damping and

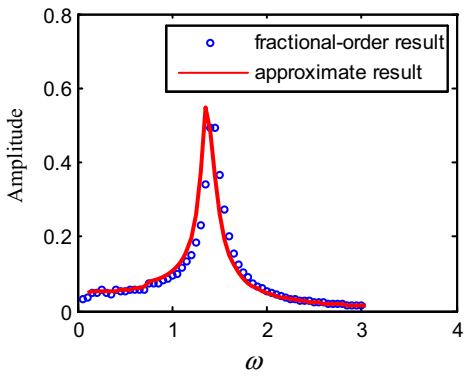

(k=1, c=0.1, α=0.1, f=0.1, λ =0.1, p=0.5 and τ =0.2)

Fig. 1 The amplitude–frequency curves

equivalent linear stiffness. Using the concepts of equivalent linear damping and equivalent linear stiffness to rearrange Eq. (10), we can get

$$\ddot{x} - \left[k - \lambda\omega^p \cos\left(\frac{p\pi}{2} - \omega\tau\right)\right] x + \left[c + \lambda\omega^{p-1} \times \sin\left(\frac{p\pi}{2} - \omega\tau\right)\right] \dot{x} + \alpha x^{33} = f\cos(\omega t) \tag{11}$$

Use the following transformations:

$$c + \lambda\omega^{p-1} \sin\left(\frac{p\pi}{2} - \omega\tau\right) = \varepsilon\left[c_1 + \lambda_1\omega^{p-1} \sin\left(\frac{p\pi}{2} - \omega\tau\right)\right] \tag{12a}$$

$$f = \varepsilon f_1 \tag{12b}$$

and Eq. (11) becomes

$$\ddot{x} - \left[k - \lambda\omega^p \cos\left(\frac{p\pi}{2} - \omega\tau\right)\right] x + \alpha x^3 = \varepsilon\left\{f_1 \cos(\omega t) - \left[c_1 + \lambda_1\omega^{p-1} \sin\left(\frac{p\pi}{2} - \omega\tau\right)\right] \dot{x}\right\} \tag{13}$$

Supposing ε is zero, the undisturbed system is

$$\ddot{x} - \left[k - \lambda\omega^p \cos\left(\frac{p\pi}{2} - \omega\tau\right)\right] x + \alpha x^3 = 0 \tag{14}$$

Here is a heteroclinic orbit in Eq. (14) which satisfies

$$\frac{1}{2}\dot{x}^2 - \frac{k - \omega^p \cos\left(\frac{p\pi}{2} - \omega\tau\right)}{2} x^2 + \frac{\alpha}{4} x^4 = 0 \tag{15}$$

Supposing $\dot{x} = 0$ at $t = 0$, one could obtain

$$x_0 = \pm\sqrt{\frac{2[k - \lambda\omega^p \cos(\frac{p\pi}{2} - \omega\tau)]}{\alpha}} \tag{16}$$

After some integral manipulations, Eq. (15) can be rewritten as follows

$$\int_{x_0}^{x} \frac{\mathrm{d}x}{\pm\sqrt{[k - \lambda\omega^p \cos(\frac{p\pi}{2} - \omega\tau)]x^2 - \frac{\alpha}{2}x^4}} = t \tag{17}$$

Calculating Eq. (17), one could get

$$x^{\pm(t)} = \pm\sqrt{\frac{2[k - \lambda\omega^p \cos(\frac{p\pi}{2} - \omega\tau)]}{\alpha}} \sec h \left[\sqrt{k - \lambda\omega^p \cos\left(\frac{p\pi}{2} - \omega\tau\right)} t\right] \tag{18}$$

Then Eq. (13) is transformed into

$$\vec{\dot{x}} = \vec{f}(\vec{x}) + \varepsilon\vec{g}(\vec{x}, t) \tag{19a}$$

where

$$\vec{x} = \begin{pmatrix} x_1 \\ x_2 \end{pmatrix} = \begin{pmatrix} x \\ \dot{x} \end{pmatrix} \tag{19b}$$

$$\vec{f}(\vec{x}) = \begin{pmatrix} x_2 \\ [k - \lambda\omega^p \cos(\frac{p\pi}{2} - \omega\tau)]x_1 - \alpha x_1^3 \end{pmatrix} \tag{19c}$$

$$\vec{g}(\vec{x}, t) = \varepsilon\begin{bmatrix} 0 \\ f_1 \cos(\omega t) - [c_1 + \lambda_1\omega^{p-1} \sin(\frac{p\pi}{2} - \omega\tau)]x_2 \end{bmatrix} \tag{19d}$$

The expression of displacement in homoclinic orbit is

$$x_1^{\pm}(t) = \pm\sqrt{\frac{2[k - \lambda\omega^p \cos(\frac{p\pi}{2} - \omega\tau)]}{\alpha}} \times \mathrm{sech}\left[\sqrt{k - \lambda\omega^p \cos\left(\frac{p\pi}{2} - \omega\tau\right)} t\right] \tag{20}$$

The velocity expression of homoclinic orbit is obtained through the derivative of Eq. (20) about$t$, and it is

$$x_2^{\pm}(t) = \mp\sqrt{\frac{2}{\alpha}}\left[k - \lambda\omega^p \cos\left(\frac{p\pi}{2} - \omega\tau\right)\right] \times \mathrm{sech}\left[\sqrt{k - \lambda\omega^p \cos\left(\frac{p\pi}{2} - \omega\tau\right)} t\right] \cdot \tanh\left[\sqrt{k - \lambda\omega^p \cos\left(\frac{p\pi}{2} - \omega\tau\right)} t\right] \tag{21}$$

According to Melnikov method [31], the Melnikov function could be established

$$M(t_0) = \vec{f}(\vec{x}) \wedge \vec{g}(\vec{x}, t) = \varepsilon \int_{-\infty}^{\infty} x_2^{\pm}(t) \Bigg\{ f_1 \cos\omega(t+t_0) - \Bigg[c_1 + \lambda_1 \omega^{p-1} \times \sin\left(\frac{p\pi}{2} - \omega\tau\right) \Bigg] x_2^{\pm}(t) \Bigg\} \mathrm{d}t \tag{22}$$

The integral in the above formula is divided into two parts and the two parts are calculated respectively. We can get

$$\begin{aligned} M_1(t_0) &= \varepsilon \int_{-\infty}^{\infty} x_2^{\pm}(t) f_1 \cos[\omega(t+t_0)] \mathrm{d}t \\ &= \mp\sqrt{\frac{2}{\alpha}}\varepsilon \left[k - \lambda\omega^p \cos\left(\frac{p\pi}{2} - \omega\tau\right)\right] \\ &\quad \times f_1 \cdot \int_{-\infty}^{\infty} \sec h \left[\sqrt{k - \lambda\omega^p \cos\left(\frac{p\pi}{2} - \omega\tau\right)}\, t\right] \\ &\quad \cdot \tanh\left[\sqrt{k - \lambda\omega^p \cos\left(\frac{p\pi}{2} - \omega\tau\right)}\, t\right] \\ &\quad \times \cos\omega(t+t_0) \mathrm{d}t \end{aligned} \tag{23a}$$

Then, according to the odevity of function, Eq. (23a) is transformed into

$$\begin{aligned} & M_1(t_0) \\ &= \pm\varepsilon\sqrt{\frac{2}{\alpha}} \left[k - \lambda\omega^p \cos\left(\frac{p\pi}{2} - \omega\tau\right)\right] f_1 \sin(\omega t_0) \\ &\quad \times \int_{-\infty}^{\infty} \sec h \left[\sqrt{k - \lambda\omega^p \cos\left(\frac{p\pi}{2} - \omega\tau\right)}\, t\right] \\ &\quad \cdot \tanh\left(\sqrt{k - \lambda\omega^p \cos\left(\frac{p\pi}{2} - \omega\tau\right)}\, t\right) \sin\omega t \mathrm{d}t \\ &= \pm\varepsilon\sqrt{\frac{2}{\alpha}} f_1 \omega\pi \sin(\omega t_0) \sec h \\ &\quad \times \left[\frac{\pi\omega}{2\sqrt{k - \lambda\omega^p \cos(\frac{p\pi}{2} - \omega\tau)}}\right] \end{aligned} \tag{23b}$$

$$\begin{aligned} & M_2(t_0) \\ &= -\varepsilon \left[c_1 + \lambda_1 \omega^{p-1} \sin\left(\frac{p\pi}{2} - \omega\tau\right)\right] \int_{-\infty}^{\infty} \left[x_2^{\pm}(t)\right]^2 \mathrm{d}t \\ &= -\frac{4\varepsilon}{3\alpha} \left[c_1 + \lambda\omega^{p-1} \sin\left(\frac{p\pi}{2} - \omega\tau\right)\right] \\ &\quad \cdot \left[k - \lambda\omega^p \cos\left(\frac{p\omega}{2} - \omega\tau\right)\right] \\ &\quad \times \sqrt{k - \lambda\omega^p \cos\left(\frac{p\pi}{2} - \omega\tau\right)} \end{aligned} \tag{23c}$$

Combine Eqs. (22) and (23), then the necessary condition for the chaos in the system will be obtained

$$\begin{aligned} & \sqrt{\frac{2}{\alpha}}\varepsilon f_1 \pi\omega \sec h \left[\frac{\pi\omega}{2\sqrt{k - \lambda\omega^p \cos(\frac{p\pi}{2} - \omega\tau)}}\right] \\ &> \left| -\frac{4\varepsilon}{3\alpha} \left[c_1 + \lambda_1 \omega^{p-1} \sin\left(\frac{p\pi}{2} - \omega\tau\right)\right] \right. \\ &\quad \cdot \left[k - \lambda\omega^p \cos\left(\frac{p\pi}{2} - \omega\tau\right)\right] \\ &\quad \left. \times \sqrt{k - \lambda\omega^p \cos\left(\frac{p\pi}{2} - \omega\tau\right)} \right| \end{aligned} \tag{24a}$$

Substitute the parameters of Eq. (12) into Eq. (24a), then we can get

$$\begin{aligned} & \sqrt{\frac{2}{\alpha}} f\omega \sec h \left[\frac{\pi\omega}{2\sqrt{k - \lambda\omega^p \cos(\frac{p\pi}{2} - \omega\tau)}}\right] > \left| -\frac{4}{3\alpha} \right. \\ &\quad \times \left[c + \lambda\omega^{p-1} \sin\left(\frac{p\pi}{2} - \omega\tau\right)\right] \\ &\quad \cdot \left[k - \lambda\omega^p \cos\left(\frac{p\pi}{2} - \omega\tau\right)\right] \\ &\quad \left. \times \sqrt{k - \lambda\omega^p \cos\left(\frac{p\pi}{2} - \omega\tau\right)} \right| \end{aligned} \tag{24b}$$

The absolute value symbol in Eq. (24b) can be removed when the equivalent stiffness produced by fractional-order term is less than the inherent stiffness of the system. Finally, the necessary conditions for chaos in Duffing system are obtained.

$$\begin{aligned} & \sqrt{\frac{2}{\alpha}} f\omega \sec h \left[\frac{\pi\omega}{2\sqrt{k - \lambda\omega^p \cos(\frac{p\pi}{2} - \omega\tau)}}\right] \\ &> \frac{4}{3\alpha} \left[c + \lambda\omega^{p-1} \sin\left(\frac{p\pi}{2} - \omega\tau\right)\right] \\ &\quad \cdot \left[k - \lambda\omega^p \cos\left(\frac{p\pi}{2} - \omega\tau\right)\right] \\ &\quad \times \sqrt{k - \lambda\omega^p \cos\left(\frac{p\pi}{2} - \omega\tau\right)} \end{aligned} \tag{25}$$

3 Numerical simulation and the influence of the fractional-order delayed feedback control on chaotic behaviors

In the previous section, the analytical necessary condition for chaos in Duffing system with fractional-order delayed feedback control is obtained based on Melnikov method. In this section, the numerical solution of the threshold for chaos of Duffing system with fractional-order delayed feedback control is studied by numerical iteration method. Then, the influence of the fractional-order delayed feedback control on chaotic behaviors is investigated.

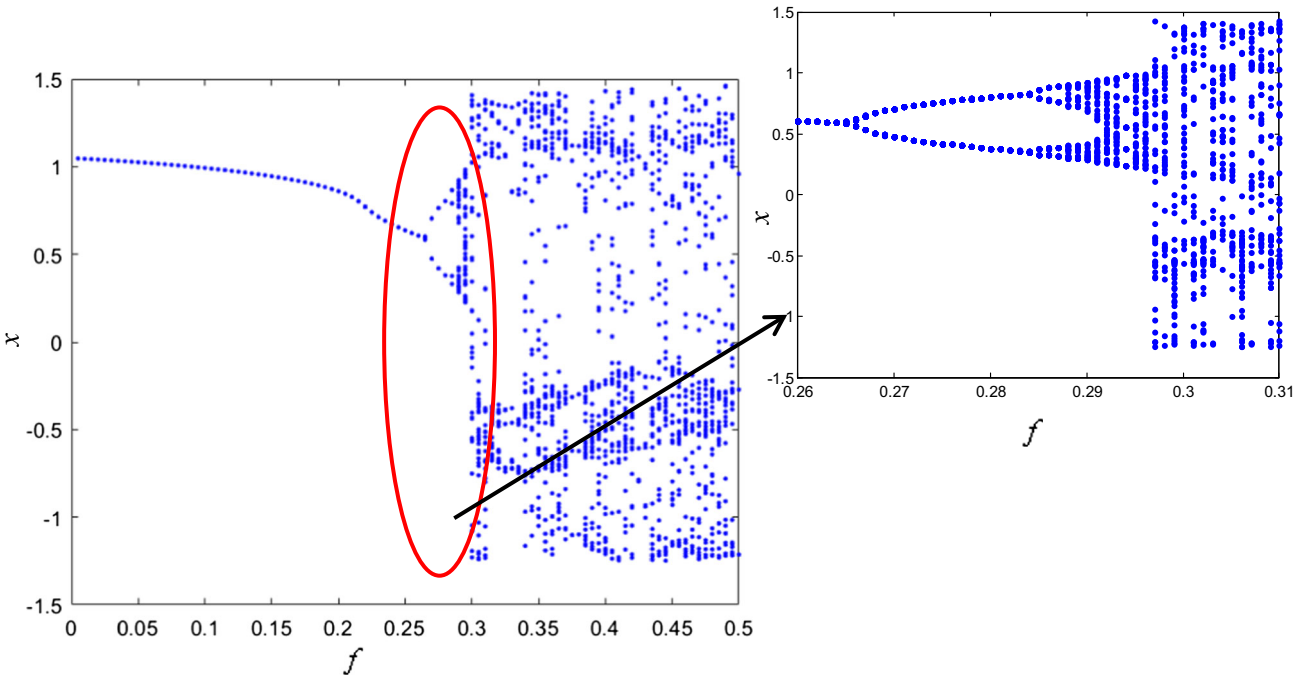

(a) Bifurcation diagram for p=0.5

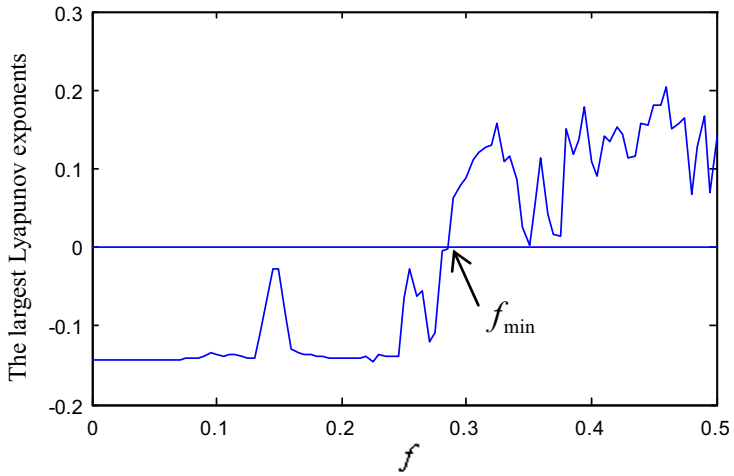

(b) The largest Lyapunov exponents diagram for p=0.5

Fig. 2 **a** Bifurcation diagram for $p = 0.5$. **b** The largest Lyapunov exponents diagram for $p = 0.5$

3.1 Numerical simulation

The numerical results of Eq. (1) are presented to verify the correctness of the analytical solution. The numerical formula [24] is

$$D^p\left[x\left(t_l\right)\right] \approx h^{-p} \sum_{j=0}^{l} C_j^p x\left(t_{l-j}\right), \tag{26}$$

where $t_l = lh$ is the time sample points, h is the sample step, C_j^p is the fractional binomial coefficient with the iterative relationship as

$$chaoticthroughperioddoublingbifurcationwiththe increaseofC_0^p = 1, C_j^p = \left(1 - \frac{1+p}{j}\right) C_{j-1}^p. \tag{27}$$

A set of system parameters are chosen as $k = 1.1$, $c = 0.25$, $\alpha = 1$, $\omega = 1.2$, $\lambda = 0.1$, $\tau = 0.2$, $p = 0.5$. The bifurcation diagram of system (1) is obtained which is shown in Fig. 1 by changing the excitation amplitude f from 0 to 0.5 and selecting the step size as 0.005. To get the more detailed result, the step size is selected as 0.001 and the local view of the bifurcation diagram is shown in Fig. 1a too. The corresponding

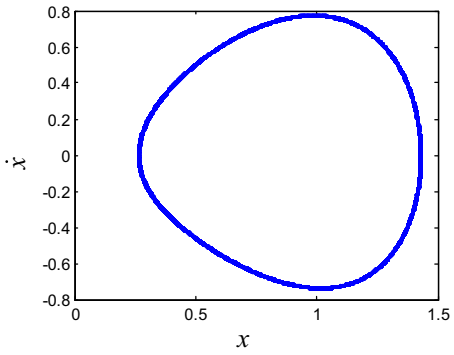

(a1) Phase portrait of f=0.26 and p=0.5

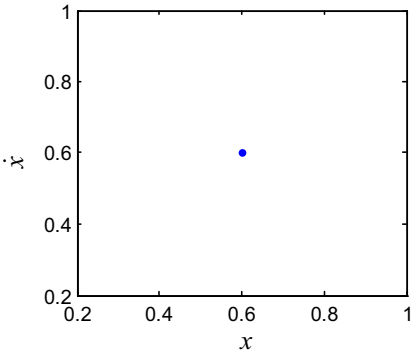

(a2) Poincaré map of f=0.26 and p=0.5

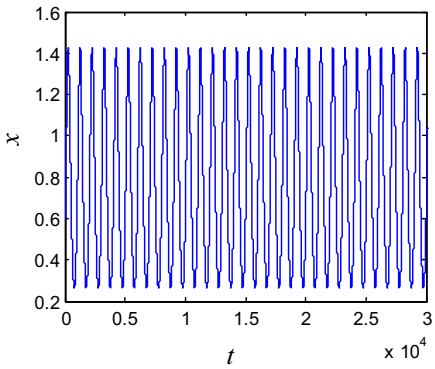

(a3) Time history of f=0.26 and p=0.5

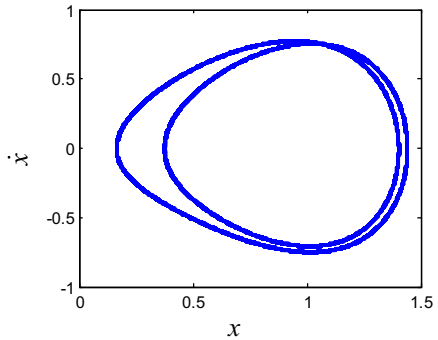

(b1) Phase portrait of f=0.275 and p=0.5

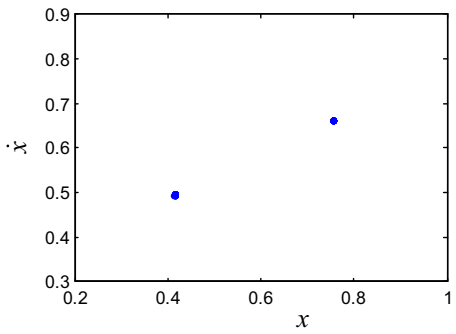

(b2) Poincaré map of f=0.275 and p=0.5

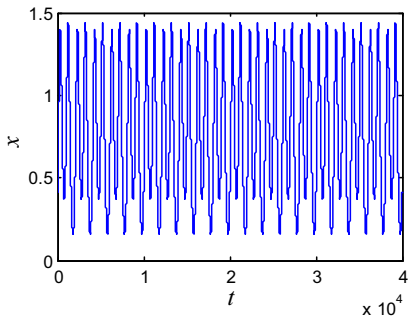

(b3) Time history of f=0.275 and p=0.5

Fig. 3 **a1** Phase portrait of $f = 0.26$ and $p = 0.5$. **a2** Poincaré map of $f = 0.26$ and $p = 0.5$. **a3** Time history of $f = 0.26$ and $p = 0.5$. **b1** Phase portrait of $f = 0.275$ and $p = 0.5$. **b2** Poincaré map of $f = 0.275$ and $p = 0.5$. **b3** Time history of $f = 0.275$ and $p = 0.5$. **c1** Phase portrait of $f = 0.285$ and $p = 0.5$. **c2** Poincaré map of $f = 0.285$ and $p = 0.5$. **c3** Time history of $f = 0.285$ and $p = 0.5$. **d1** Phase portrait of $f = 0.296$ and $p = 0.5$. **d2** Poincaré map of $f = 0.296$ and $p = 0.5$. **d3** Time history of $f = 0.296$ and $p = 0.5$. **e1** Phase portrait of $f = 0.297$ and $p = 0.5$. **e2** Poincaré map of $f = 0.297$ and $p = 0.5$. **e3** Time history of $f = 0.297$A and $p = 0.5$

Fig. 3 continued

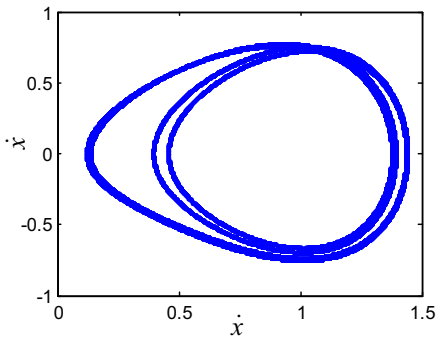

(c1) Phase portrait of f=0.285 and p=0.5

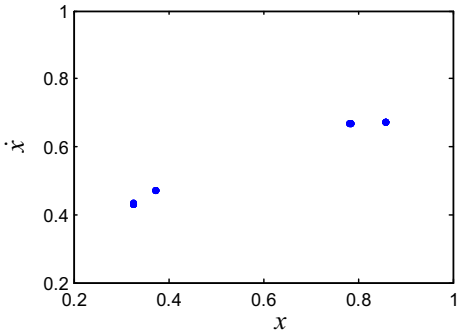

(c2) Poincaré map of f=0.285 and p=0.5

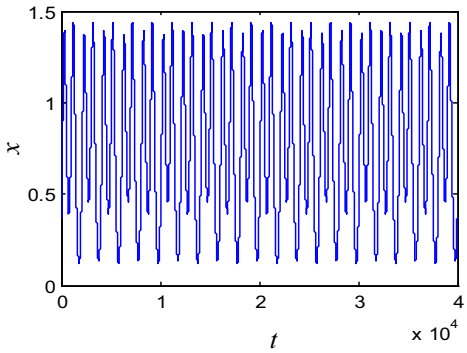

(c3) Time history of f=0.285 and p=0.5

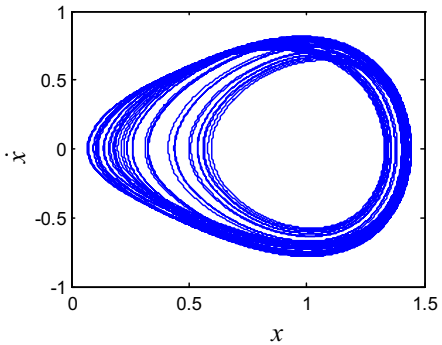

(d1) Phase portrait of f=0.296 and p=0.5

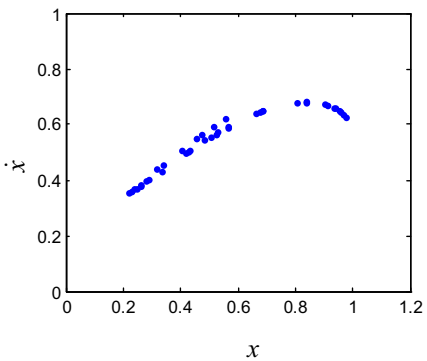

(d2) Poincaré map of f=0.296 and p=0.5

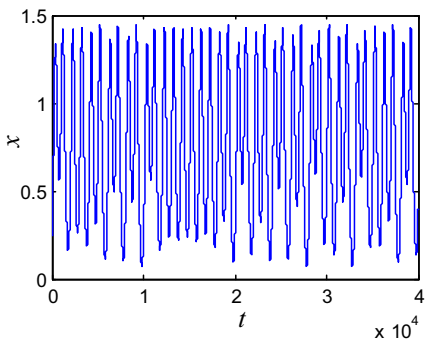

(d3) Time history of f=0.296 and p=0.5

Fig. 3 continued

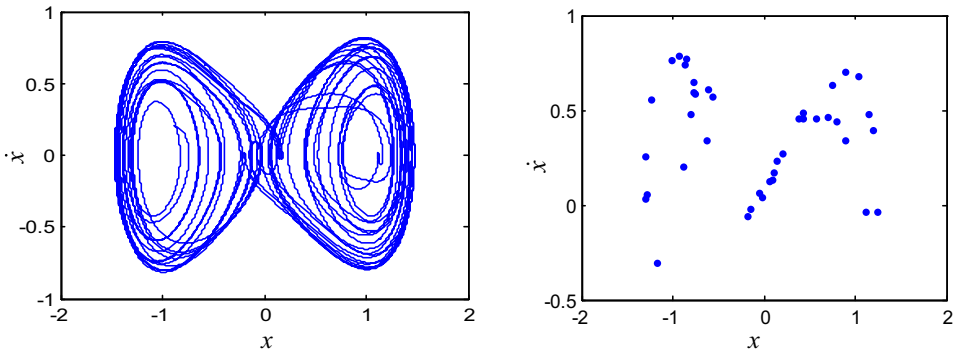

(e1) Phase portrait of f=0.297 and p=0.5

(e2) Poincaré map of f=0.297 and p=0.5

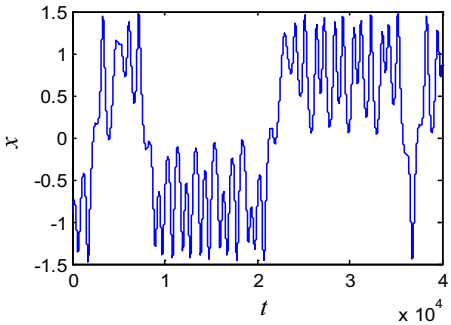

(e3) Time history of f=0.297 and p=0.5

largest Lyapunov exponents are shown in Fig. 1b, and it can be seen from Fig. 2 that the critical excitation amplitude $f_{\min}$ for generating chaos is around 0.3.

From Fig. 2, it is periodic motion when f is small, but becomes chaotic through period-doubling bifurcation with the increase of the excitation amplitude f. Some typical samples in different ranges are taken to analyze the dynamical motion.

1. The dynamical motion of the system is period-1 when $f \leq 0.264$. Supposing $f = 0.26$, the phase portrait, time history and Poincaré maps are shown in Fig. 3a.
2. When $f \in [0.265, 0.283]$, the dynamical motion of system is period-2. Supposing $f = 0.275$ in this range, the phase portrait, time history and Poincaré maps are shown in Fig. 3b.
3. When $f \in [0.284, 0.287]$, the dynamical motion of system is period-4. Supposing $f = 0.285$ in this range,the phase portrait, time history and Poincaré maps are shown in Fig. 3c.
4. In the range of $f \in [0.288, 0.296]$ and $f \geq 0.297$, supposing $f = 0.296$ and $f = 0.297$, respectively. The phase portrait, time history and Poincaré maps of the system under the two parameters are shown in Fig. 3d, e respectively. From Fig. 3e, it could be found that the motion orbit of the phase trajectory is homoclinic orbit and the mapping points in the Poincaré maps are disordered, so the system is completely in chaos in this case. The trajectory of the phase trajectory in Fig. 3d is not in chaos. At the same time, the mapping points in the Poincaré maps show certain regularity in a sense. Therefore, it is considered that the motion state of the system at this time is quasi periodic and not completely in chaos.

Change the initial value of the system, and other parameters aren't changed. Another bifurcation path appeared, which is shown in Fig. 4 by red dots. The phase portrait, time history and Poincaré map of $f = 0.26$, $f = 0.275$, $f = 0.285$, $f = 0.296$ and $f = 0.297$ are shown in Fig. 5 respectively. The initial value of blue path is "1,0,0" and the initial value of the red path is "-1,0,0". It could be found that there are two paths leading to the chaos via different period-doubling bifurcation. The system dynamical motion are shown in Fig. 5a–e, respectively, with the different f.

The comparison between the two paths shows that the positions of bifurcations are the same. So the critical value of chaos will not change by changing the initial value.

Compare Fig. 3a with Fig. 5a, Fig. 3b with Fig. 5b, Fig. 3c with Fig. 5c and Fig. 3e with Fig. 5e, and it shows that the position of the phase diagram in periodic motion will change due to different initial values. The two phase diagrams are the left and right half of the phase diagram in chaos respectively, but the motion characteristic of the system will not change because of two different domains of attraction in the phase space of Duffing system under fractional-order feedback coupling with time delay. When the initial values are differ-

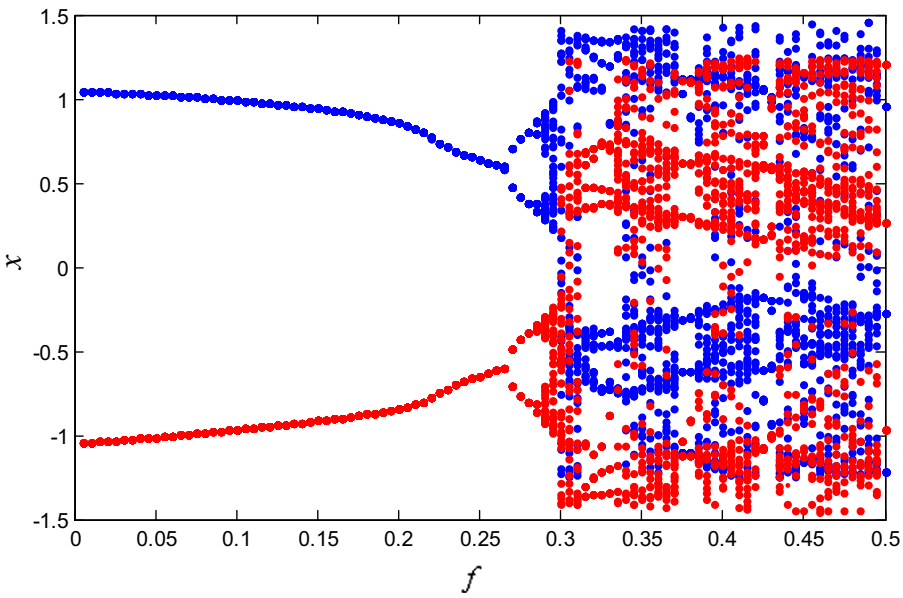

(a) Bifurcation diagram for p=0.5(in different initial value)

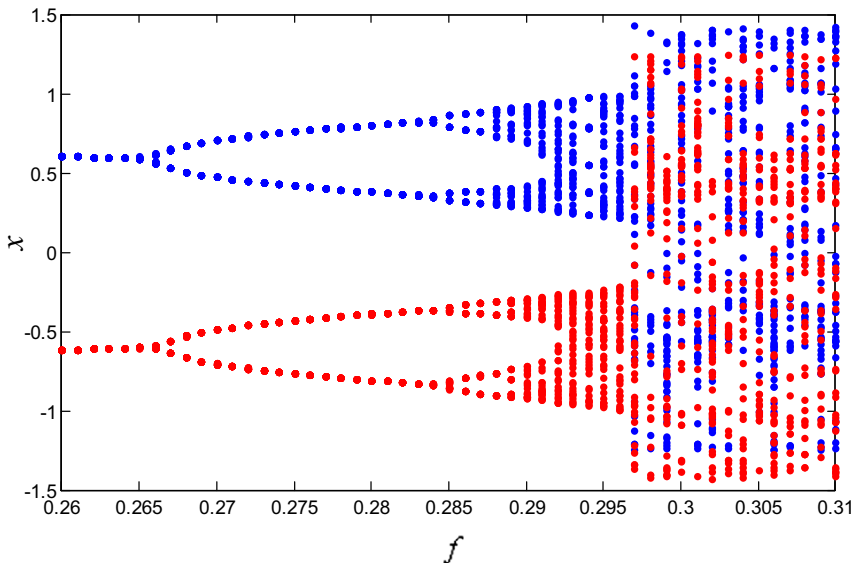

(b) Bifurcation diagram for p=0.5(Local view)

Fig. 4 **a** Bifurcation diagram for $p = 0.5$ (in different initial value). **b** Bifurcation diagram for $p = 0.5$A (local view)

ent, the system will enter the different domain of attraction and form different steady-state solutions. When the system is in a single period state, there are two steady-state solutions. With the change of the external excitation amplitude, both the two steady-state solutions can reach the chaos through period-doubling bifurcation.

3.2 The comparison of two methods and the effect of the fractional order

The same system parameters $k = 1.1$, $c = 0.25$, $\alpha = 1$, $\omega = 1.2$, $\lambda = 0.1$, $\tau = 0.2$, $p = 0.5$ are substituted into Eq. (25) which is the analytical necessary condition for chaos threshold in Duffing system, then one can get the critical excitation amplitude $f_{\min} = 0.250$. Comparing with the numerical result $f_{\min} = 0.297$, we could find there is some error. As is known to all, the obtained analytical necessary condition by Melnikov method is the first-order approximate result, so there are errors in the method itself. The relation curve between the excitation amplitude $f_{\min}$ and fractional order p of system (1) can be obtained by changing the fractional order p from 0 to 2, which is represented by a solid line in Fig. 6, and the numerical simulation results are shown by small circle in Fig. 6 too. By comparing the results of the two methods, we can see that the necessary condition of chaos by the analytical solution is smaller than the numerical solution. But the tendency of analytical results is similar to the numerical simulation results, so

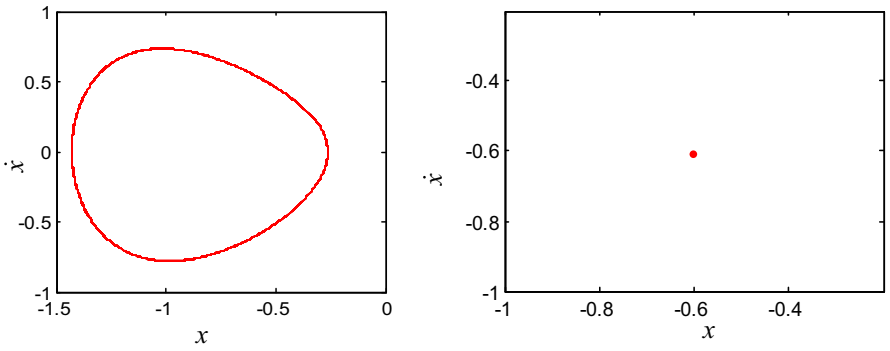

(a1) Phase portrait of f=0.26 and p=0.5 (a2) Poincaré map of f=0.26 and p=0.5

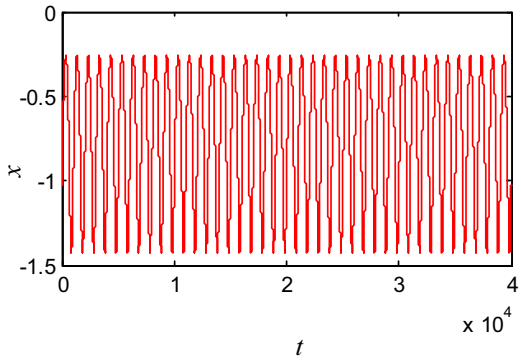

(a3) Time history of f=0.26 and p=0.5

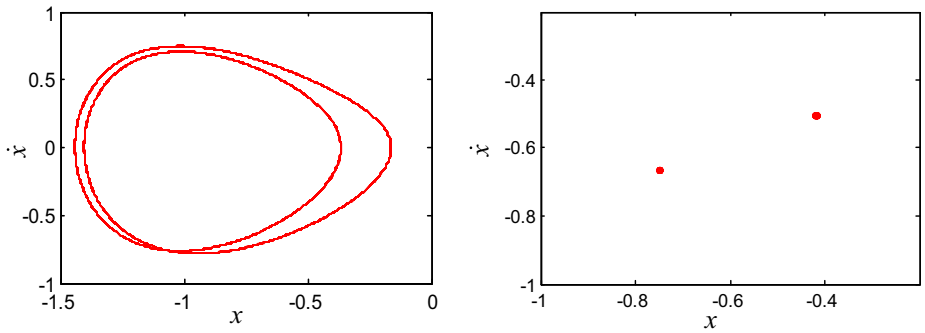

(b1) Phase portrait of f=0.275 and p=0.5 (b2) Poincaré map of f=0.275 and p=0.5

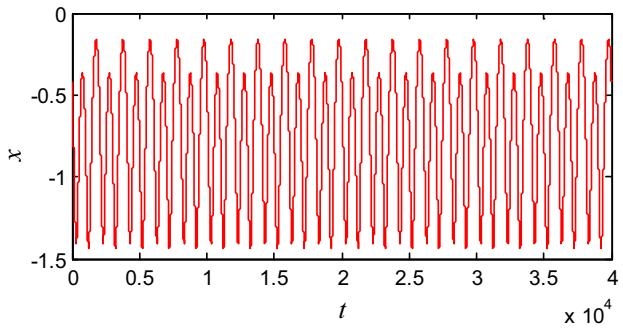

(b3) Time history of f=0.275 and p=0.5

Fig. 5 **a1** Phase portrait of $f = 0.26$ and $p = 0.5$. **a2** Poincaré map of $f = 0.26$ and $p = 0.5$. **a3** Time history of $f = 0.26$ and $p = 0.5$. **b1** Phase portrait of $f = 0.275$ and $p = 0.5$. **b2** Poincaré map of $f = 0.275$ and $p = 0.5$. **b3** Time history of $f = 0.275$ and $p = 0.5$. **c1** Phase portrait of $f = 0.285$ and $p = 0.5$. **c2** Poincaré map of $f = 0.285$ and $p = 0.5$. **c3** Time history of $f = 0.285$ and $p = 0.5$. **d1** Phase portrait of $f = 0.296$ and $p = 0.5$. **d2** Poincaré map of $f = 0.296$ and $p = 0.5$. **d3** Time history of $f = 0.296$ and $p = 0.5$. **e1** Phase portrait of $f = 0.297$ and $p = 0.5$. **e2** Poincaré map of $f = 0.297$ and $p = 0.5$. **e3** Time history of $f = 0.297$ and $p = 0.5$

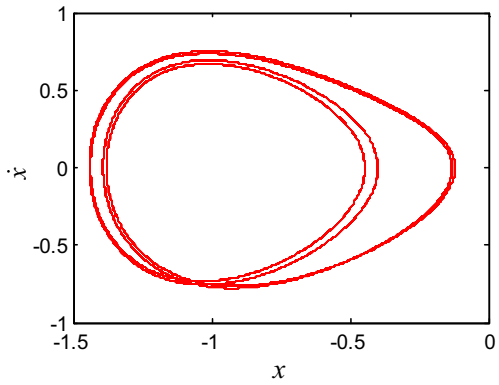

(c1) Phase portrait of f=0.285 and p=0.5

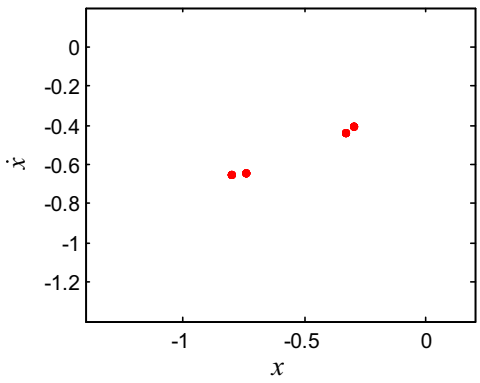

(c2) Poincaré map of f=0.285 and p=0.5

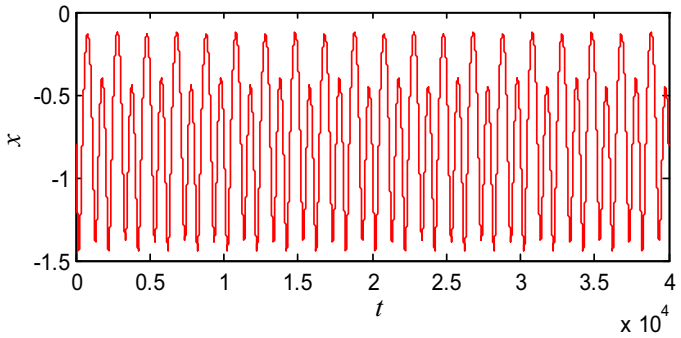

(c3) Time history of f=0.285 and p=0.5

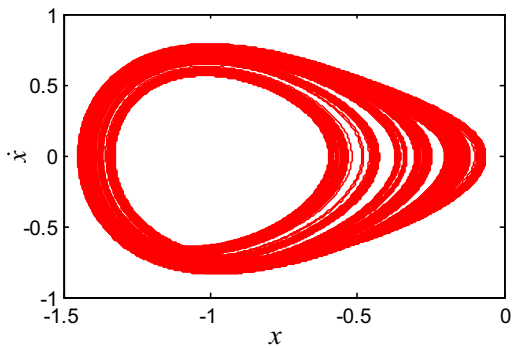

(d1) Phase portrait of f=0.296 and p=0.5

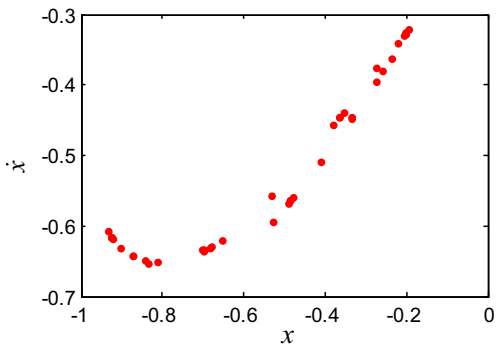

(d2) Poincaré map of f=0.296 and p=0.5

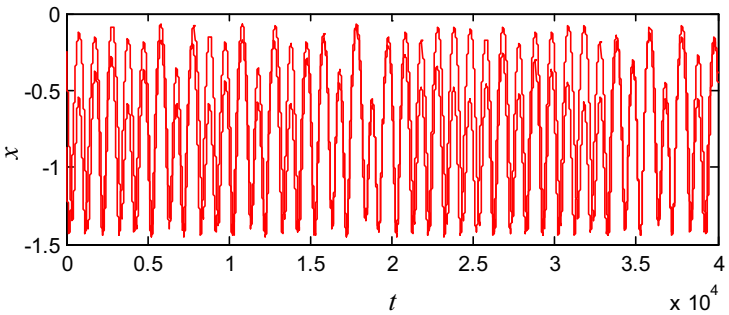

(d3) Time history of f=0.296 and p=0.5

Fig. 5 continued

Fig. 5 continued

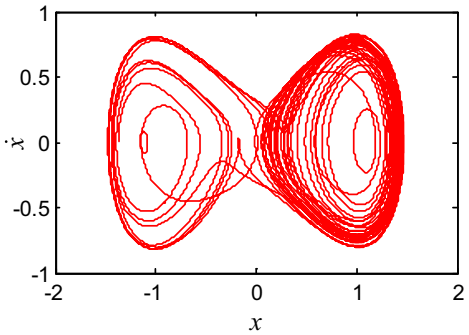

(e1) Phase portrait of f=0.297 and p=0.5

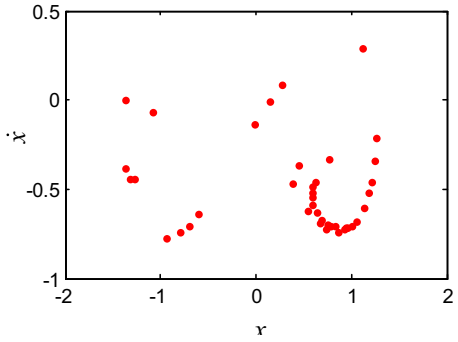

(e2) Poincaré map of f=0.297 and p=0.5

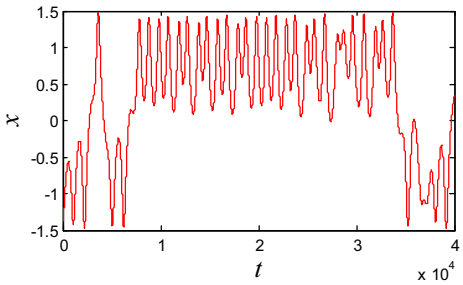

(e3) Time history of f=0.297 and p=0.5

the results of the two methods are consistent qualitatively.

From the observation of Fig. 6, it could be obtained that increase of p would make the chaos threshold value first increase then decrease, and $f_{\min}$ reaches the maximum value when p is 1.144. Through analyzing Eq. (25), when time delay is zero, it could be obtained that the equivalent linear stiffness decreases and the equivalent linear damping increases when the fractional order $p$changed from 0 to 1, but the equivalent linear stiffness increases and the equivalent linear damping decreases when the fractional order $p$changed from 1 to 2. From Fig. 6, we found $f_{\min}$ reaches the maximum, the fractional order p is greater than 1 that is because there exists time delay. Time delay will affect the system stiffness and damping and it would cause the peak of $f_{\min}$ move to the right. So when time delay is small, selecting the fractional order properly can resist the generation of chaos.

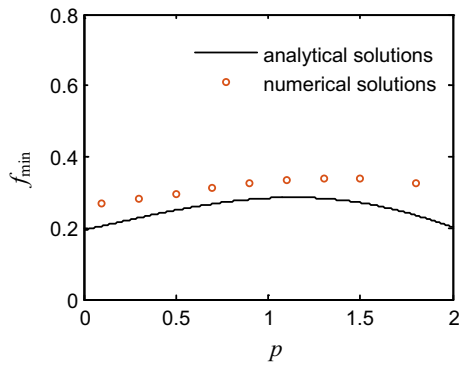

Fig. 6 The comparisons between the numerical and analytical solutions

3.3 The effect of the fractional-order delayed feedback gain

A set of illustrative system parameters are chosen as $k = 1.1$, $c = 0.25$, $\alpha = 1$, $\omega = 1.2$, $\tau = 0.2$. The fractional order p is changed from 0 to 2. The corresponding p and $f_{\min}$ curves are obtained by chosen different values of the fractional-order delayed feedback gain λ, and the results are shown in Fig. 7. From the observation of Fig. 7, it could be found that the excitation amplitude $f_{\min}$ for generating chaos will become larger with the increase of λ. When p is small or large, the rate of $f_{\min}$ change is not obvious. When p is around 1, the rate of $f_{\min}$ change is larger. In summary, the increase of the fractional-order delayed feedback gain λ can resist the generation of chaos.

3.4 The effect of time delay

The same system parameters are chosen. The corresponding p and $f_{\min}$ curves are obtained by choosing different values of time delay τ, which is shown in Fig. 8. From the observation of Fig. 8, it could be found that the increase of time delay τ would result in the decrease of $f_{\min}$ when the fractional order p changed from 0 to 1. The increase of time delay τ would result into the increase of $f_{\min}$ when the fractional order p is close to 2. When p is around 1, the rate of $f_{\min}$ change is smaller. That is to say, the maximum of $f_{\min}$ is basically the same with different p. It shows that the change of time delay can be offset by choosing the different p. It

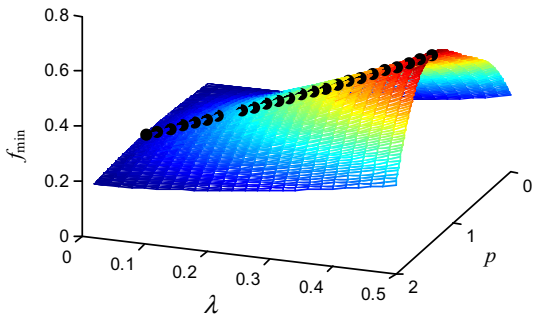

Fig. 7 The influence of fractional-order delayed feedback gain

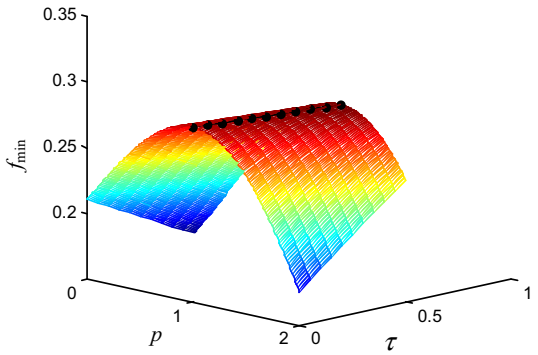

Fig. 8 The influence of time delay

can also be seen from the composition of Eq. (25), both time delay and the fractional order affect the threshold of chaos in the form of trigonometric functions. Therefore, the magnitude of the time delay in fractional-order feedback control has an important influence on the stability of the system.

4 Conclusion

A Duffing system with fractional-order delayed feedback is studied by the Melnikov method in this paper. Firstly, the fractional-order delayed feedback control is studied and replaced with integer-order term equivalently. By defining the equivalent linear stiffness and the equivalent linear damping, the fractional-order delayed feedback control is transformed into the equivalent linear stiffness and the equivalent linear damping. Then, the Melnikov method is used to study the analytically necessary condition of the equivalent system for generating chaos. To validate the accuracy of the proposed analytical method, the numerical results of the Eq. (1) are solved based on numerical iteration method and the corresponding largest Lyapunov exponents are obtained, then the comparison between the numerical results and the analytical solution is investigated. From the analysis of numerical simulations, it could be found that there exist two paths leading to chaos via period-doubling bifurcation in Duffing system with fractional-order delayed feedback control. Finally, the effects of the fractional order, the gain coefficient and time delay are studied respectively. The fractional order, the gain coefficient and time delay all can affect the equivalent linear stiffness and the equivalent linear damping. The increase of the fractional order will make the chaos threshold value increase before decrease, and the increase of the gain coefficient can resist the generation of chaos. Also, both time delay and the fractional order affect the threshold of chaos in the form of trigonometric functions, so the change of time delay can be offset by choosing the different fractional order. These results are of great significance to the study of the dynamic behavior of control system. They can provide a reference for the analysis of other fractional-order differential systems with time delay, and provide a theoretical analysis method for the design of the fractional-order system in engineering practice.

Acknowledgements The authors are grateful for the support by National Natural Science Foundation of China (12072206, U1934201, 11802183), the Natural Science Foundation of Hebei Province (E2018210056), the Education Department Project of Hebei Province (ZD2020310).

References

1. Y. Bolotin, A. Tur, V. Yanovsky, *Chaos: Concepts, Control and Constructive Use* (Springer International Publishing, Cham, 2017)
2. J.L. Mccauley, *Nonlinear Dynamics and Chaos Theory* (Royal Swedish Academy of Sciences Press, Stockholm, 1991)
3. E. Ott, C. Grebogi, J.A. Yorke, Controlling chaos. Phys. Rev. Lett. **64**(11), 1796–1799 (1990)
4. J.H. Li, H.B. Wu, N. Cui, Bifurcation, chaos, and their control in a wheelset model. Math. Methods Appl. Sci. **43**(12), 7152–7174 (2020)
5. A. Saghafi, A. Farshidianfar, An analytical study of controlling chaotic dynamics in a spur gear system. Mech. Mach. Theory **96**, 179–191 (2016)
6. E. Shiva, K.G. Reza, A. Alireza, Hopf bifurcation, chaos control and synchronization of a chaotic fractional-order system with chaos entanglement function. Math. Comput. Simul. **172**, 321–340 (2020)
7. Y.G. Wang, X.P. Zhang, L.P. Yang, H. Huang, Adaptive synchronization of time delay chaotic systems with uncertain and unknown parameters via aperiodically intermittent control. Int. J. Control Autom. Syst. **18**, 696–707 (2020)
8. M.Y. Chen, Z.Z. Han, Controlling and synchronizing chaotic Genesio system via nonlinear feedback control. Chaos Solitons Fract. **17**(4), 709–716 (2003)
9. H.Y. Hu, Z.H. Wang, Stability analysis of damped SDOF systems with two time delays in state feedback. J. Sound Vib. **214**(2), 213–225 (1998)
10. J.P. Richard, Time-delay systems: an overview of some recent advances and open problems. Automatica **39**(10), 1667–1694 (2003)

11. Z.M. Ge, C.L. Hsiao, Y.S. Chen, Nonlinear dynamics and chaos control for a time delay Duffing system. Int. J. Nonlinear Sci. Numer. Simul. **6**(2), 187–199 (2005)
12. X. Xu, H.Y. Hu, H.L. Wang, Stability, bifurcation and chaos of a delayed oscillator with negative damping and delayed feedback control. Nonlinear Dyn. **49**(1–2), 117–129 (2007)
13. Z.H. Wang, Numerical Stability test of neutral delay differential equations. Math. Probl. Eng. **698043**, 1–10 (2008)
14. R. Hu, Almost sure exponential stability of the Milstein-type schemes for stochastic delay differential equations. Chaos Solitons Fract. **131**(109499), 1–8 (2020)
15. J.E. Marshall, H. Gorecki, K. Walton, W. Korytowski, *Time-Delay Systems: Stability and Performance Criteria with Applications* (Ellis Horwood, New York, 1992)
16. Y. Yu, Z.D. Zhang, Q.S. Bi, Multistability and fast-slow analysis for Van der Pol–Duffing oscillator with varying exponential delay feedback factor. Appl. Math. Model. **57**, 448–458 (2018)
17. J. Xu, K.W. Chung, Effects of time delayed position feedback on a Van der Pol–Duffing oscillator. Phys. D **180**(1), 17–39 (2003)
18. C.S. Feng, W.Q. Zhu, First-passage failure of harmonically and stochastically excited Duffing oscillator with delayed feedback control. Sci. China Technol. Sci. **54**, 1072–1077 (2011)
19. C.H. Cai, Z.Y. Xu, W.B. Xu, Melnikov's analysis of time-delayed feedback control in chaotic dynamics. IEEE Trans. Circuits Syst. I Fundam. Theory Appl. **49**(12), 1724–1728 (2002)
20. Z.K. Sun, W. Xu, X.L. Yang, Including or suppressing chaos in a double-well Duffing oscillator by time delay feedback. Chaos Solitons Fract. **27**, 705–714 (2006)
21. Y.J. Shen, S.P. Yang, H.J. Xing, H.X. Ma, Primary resonance of Duffing oscillator with two kinds of fractional-order derivatives. Int. J. Non-Linear Mech. **47**(9), 975–983 (2012)
22. T. Pirbodaghi, S.H. Hoseini, M.T. Ahmadian, G.H. Farrahi, Duffing equations With cubic and quintic nonlinearities. Comput. Math. Appl. **57**(3), 500–506 (2009)
23. A. Raghda, L. Dianchen, K.M.A. Mostafa, Chaos and relativistic energy–momentum of the nonlinear time fractional Duffing equation. Math. Comput. Appl. **24**(1), 10 (2019)
24. I. Petras, *Fractional-Order Nonlinear System* (Higher Education Press, Beijing, 2011)
25. B. Ross, *A Brief History and Exposition of the Fundamental Theory of Fractional Calculus* (Springer, Berlin, 1974)
26. R. Caponetto, I. Ebrary, *Fractional Order Systems: Modeling and Control Applications* (World Scientific, Singapore, 2010)
27. A.M. Akbar, A.N.H. Mohd, R. Ripan, Closed form solutions of two time fractional nonlinear wave equations. Results Phys. **9**, 1031–1039 (2018)
28. R.M. Wang, Y.N. Zhang, Y.Q. Chen, X. Chen, L. Xi, Fuzzy neural network-based chaos synchronization for a class of fractional-order chaotic systems: an adaptive sliding mode control approach. Nonlinear Dyn. **100**(4), 1275–1287 (2020)
29. Y.H. Wei, D. Sheng, Y.Q. Chen, Y. Wang, Fractional-order chattering-free robust adaptive backstepping control technique. Nonlinear Dyn. **95**, 2383–2394 (2019)
30. L.P. Chen, R.C. Wu, Y.G. He, Y. Chai, Adaptive sliding-mode control for fractional-order uncertain linear systems with nonlinear disturbances. Nonlinear Dyn. **80**(1–2), 51–58 (2015)
31. J. Guckenheimer, P. Holmes, *Nonlinear Oscillations, Dynamical System and Bifurcations of Vector Fields* (Springer, New York, 1983)